Lock-in Thermography Failure Detection on Multilayer Ceramic Capacitors After Flex Cracking and Temperature-Humidity-Bias Stress

Andersson, Caroline; Kristensen, Ole; Miller, Stefanie; Gloor, Thomas; Iannuzzo, Francesco

Published in:
IEEE Journal of Emerging and Selected Topics in Power Electronics

DOI (link to publication from Publisher):
10.1109/JESTPE.2018.2866545

Publication date:
2018

Document Version
Accepted author manuscript, peer reviewed version

Lock-in Thermography Failure Detection on Multilayer Ceramic Capacitors After Flex Cracking and Temperature-Humidity-Bias Stress

Caroline Andersson, *Member, IEEE,* Ole Kristensen, Stefanie Miller, *Student Member, IEEE,* Thomas Gloor and Francesco Iannuzzo, *Senior Member, IEEE*

Abstract

A non-destructive method using lock-in thermography to detect failures in multilayer ceramic capacitors is presented. The thermal response of new 25 V multilayer ceramic capacitors is compared to the thermal response of the same capacitors after insertion of flex cracks as well as after 24 and 96 hours of total exposure time to a temperature of 75°C, 75% relative humidity, and 25 V bias. The thermal response was measured before the introduction of any flex cracks, as well as directly after flex cracks were inserted by bending the printed circuit board to 6000 μStr. No significant change was detected in the thermal profile upon introduction of flex cracks of which the presence was verified by X-ray imaging. After the multilayer ceramic capacitors were subjected to a total of 96 hours of temperature-humidity-bias stress, a significant increase in leakage current could be detected as a hotspot in one of the initially 24 samples by lock-in thermography. The influence of the different parameters, such as lock-in frequency, bias voltage and measurement time, on the detectability of the hotspot is presented.

C. Andersson, O. Kristensen and S. Miller are with the Department of Power Electronics, ABB Switzerland Ltd., Corporate Research, Baden-Dättwil, Switzerland, e-mail: caroline.andersson@ch.abb.com

T. Gloor is with Department of Quality Management, ABB Switzerland Ltd, Semiconductors, Lenzburg, Switzerland.

F. Iannuzzo is with the Department of Energy Technology, Aalborg University, CORPE, Aalborg, Denmark.

Manuscript received Month dd, 20xx; revised Month dd, 20xx.

Finally, the hotspot location is correlated with the cross-section analysis of the capacitor where melting and solidifying into nickel spheres is found.

Index Terms

Capacitors, failure analysis, infrared imaging, optical microscopy, X-rays.

I. Introduction

Multilayer ceramic capacitors (MLCCs) are often used for voltage stabilization or filtering in electronics products [1]. During manufacturing, handling and testing of printed circuit board assemblies (PCBAs), mechanical stress can result in small cracks between the opposing electrode layers in the MLCCs, which with the addition of humidity and applied voltage bias can develop into an electrical short [2], [3]. These short circuits are very detrimental and can destroy the MLCC and even the surrounding circuit [4], [5]. The flex cracks induced by bending cannot be detected by electrical measurements or identified from the surface through optical inspection [6], [7], and the resulting failure after humidity and applied voltage bias can be difficult to detect on a populated board [8], [9]. Therefore, it is desired to have a testing method to identify the leakage due to flex crack defects in a non-destructive way. Previously, it has been shown that lock-in thermography (LIT) is able to detect failures in tantalum capacitors [10] and silver migration on the surface of an MLCC [11]. Wang et. al showed that IR can be used to correlate an IR hotspot with a failure in an MLCC and linked it to impurities [12], however, to the authors' knowledge no previous attempts have been done at using this method for detection of failures in MLCCs due to flex cracks.

II. The experiment

For the experiments four test boards with a width of $10\ \mathrm{cm}$ and a length of $25\ \mathrm{cm}$ were used. The boards have each three traces containing an 1812-sized MLCC and a 2220-sized MLCC each with an X7R dielectric (see Fig. 1). The 24 MLCCs were all rated at 22 $\mu\mathrm{F}$ and 25 V, and the capacitors were having standard end terminations and soldered with Pb-free solder. A 330 Ω resistor was mounted in parallel on each of the traces in order to allow a pulsation of the voltage during the LIT measurement. Also, a $48\ \Omega$ resistor was mounted onto the PCBA to limit the current during turn-on and another $1\ \Omega$ measurement resistor. The MLCCs were mounted in a 45° orientation to the edges of the board and the resulting bending direction due to the

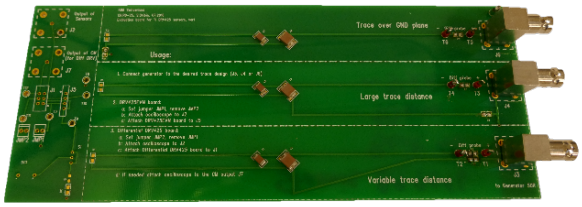

Fig. 1. Test board containing three sets of an 1812-sized and a 2220-sized MLCC in parallel on separate traces. The MLCCs are rated at 22µF, 25 V with standard end terminations. A 330 Ω resistor is mounted in parallel on each trace to allow a pulsation of the voltage.

experimental results supporting that this orientation allows the lowest bending strain levels to introduce flex cracks [13].

A. Lock-in thermography characterization

The thermal footprint of the MLCCs was measured using a LIT system consisting of a Jenoptik IR-TCM 640 thermal camera connected to a computer running the Irbis Active Online 3 software. The equivalent circuit of the test board connected to the LIT setup is shown in Fig. 2, where R_{limit} limits the current during on-state in case of an MLCC short-circuit failure, while R_{sense} allows the leakage current to be measured. $R_{parallel}$ enables the MLCCs to discharge during off-state, in order to allow a pulsation of the dissipated power. The camera is a Focal Plane Array with a spectral range from 7.5-14 µm and the frame rate was set to 50 Hz. Calibration of the camera was done by means of placing it in a climatic chamber for simulating the environmental temperatures which have a strong impact on the housing temperature and thus, of the overall radiation the detector gets. This is a compensated calibration on blackbodies which takes the housing temperature of the camera into account.

LIT is using temperature values based on object radiation and is showing temperature changes which follow the excitation frequency. A magnification lens with a magnification factor of 1.0 was used which ensures a spatial resolution of 25 µm per pixel. The numerical aperture of the lens was 1.0. The lock-in signal was provided by a simple on-off switching of a power MOSFET. As a starting point, a lock-in frequency of 1 Hz with a bias voltage of 10 V was used for the measurements with a measurement time of 3 min, these parameters were however varied later in the paper in order to examine its impact on the corresponding hotspot signal. The resulting images show the thermal footprint for the samples where the colors correspond to temperature difference

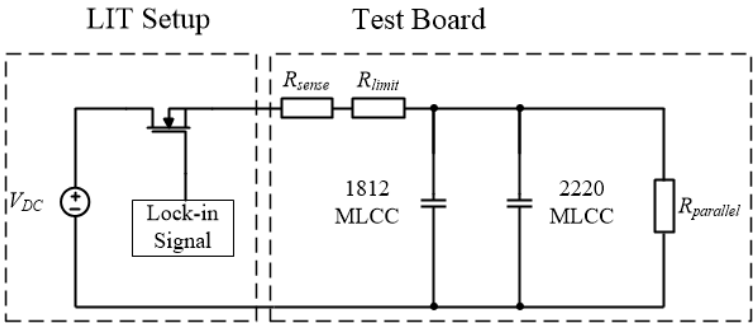

Fig. 2. Equivalent circuit of the test board connected to the LIT setup. R_{limit} limits the current during on-state in case of an MLCC short-circuit failure, while R_{sense} allows the leakage current to be measured. $R_{parallel}$ allows the MLCCs to discharge during off-state in order to allow a pulsation of the dissipated power.

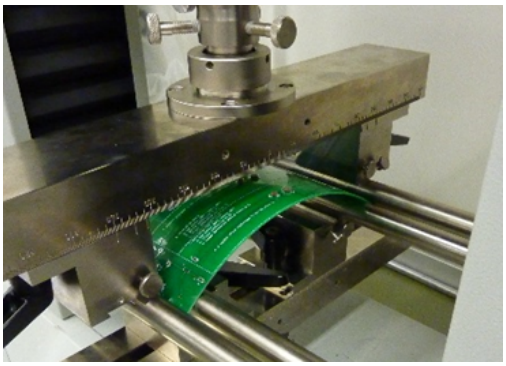

Fig. 3. Bending of the test boards to 6000 µStr using a 4-point bending setup according to IPC/JEDEC-9702A standard [16].

in mK. On the temperature scale, both negative and positive temperatures are displayed because the resulting complex image is generated by rotating the Fourier analysis result vector by the angle of the complex image and subsequent projection onto the x-axis [14], [15]. These x-values can be both negative and positive due to the mentioned rotation. It is the resulting image based on the amplitude image and the phase image which are the mathematical results of the Fourier analysis. All measurements were performed at $22^{\circ}\mathrm{C} \pm 2^{\circ}\mathrm{C}$ and 40% relative humidity $\pm$ 10%. The emissivity of the material was not corrected for in this qualitative investigation.

B. Insertion of flex cracks through mechanical bending

In order to introduce flex cracks into the MLCCs in a reproducible manner, the test boards were bent to a strain level of 6000 µStr by the use of a 4-point bending setup (see Fig. 3). The strain level was calculated using the board thickness of 1.5 mm, the distances between the

anvils and the displacement through bending according to IPC/JEDEC-9702A standard [16], as also described in [13].

C. X-ray imaging and cross-section analysis

After the bending experiments where the flex cracks were introduced in a reproducible way, the MLCCs were examined in a Phoenix Nanomex X-ray machine that has a resolution of 200 nm [17] in order to find flex cracks [13]. The settings of 160 kV and 120 $\mu\mathrm{A}$ were used for 2D imaging at a viewing angle of 70° together with the software x|act.

Using X-rays to detect cracks in MLCCs is found to be a reliable method, however, the severity of the cracks, namely if they cause a failure, cannot be estimated by this method. When using LIT, the severity of cracks can be determined by evaluation of the hotspot size, yet, a short is needed in order to obtain a hotspot. Thus, LIT can only be used for failure analysis, but not for sampling.

After X-ray, LIT and leakage current measurements, the MLCC was cross-sectioned by casting it in a two-phase epoxy and grinding the sample with a Struers Rotopol-11 to reach the desired depth of the MLCC. After polishing to ensure a scratch-free surface, the sample was inspected by a Leica M205C and a Leitz Ortholux II optical microscope and the images were recorded by the Leica Application Suite software.

D. Acceleration of flex cracks into a leakage path

In order to accelerate the humidity transport into the flex cracks to create a leakage path for the hotspot analysis, the MLCCs were exposed to temperature, humidity and bias (THB) stress using a Vötsch VC 0018 humidity chamber with 75°C, 75% relative humidity while applying the rated voltage of 25 V. In the first step the test boards were exposed to 24 hours of THB treatment, and afterwards an additional 12 of the MLCCs were exposed to another 48 hours of THB stress resulting in a total of 96 hours.

III. Results

All of the 24 investigated MLCCs showed approximately the same thermal footprint when measured with LIT before the introduction of flex cracks through bending. An example of this lock-in thermography image of an 1812-sized MLCC is shown in Fig. 4. It is observed that the active area of the MLCC is heated uniformly with a temperature increase of approximately 7 mK, and no hotspots can be detected.

This article has been accepted for publication in a future issue of this journal, but has not been fully edited. Content may change prior to final publication. Citation information: DOI 10.1109/JESTPE.2018.2866545, IEEE Journal of Emerging and Selected Topics in Power Electronics

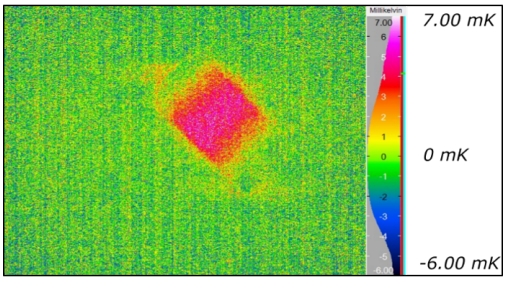

Fig. 4. Thermal footprint of a pristine 1812-sized MLCC with a uniform temperature increase of 7 mK in the capacitor body. LIT was conducted with a lock-in frequency of 1 Hz at 10 V for 3 min. No hotspot can be detected.

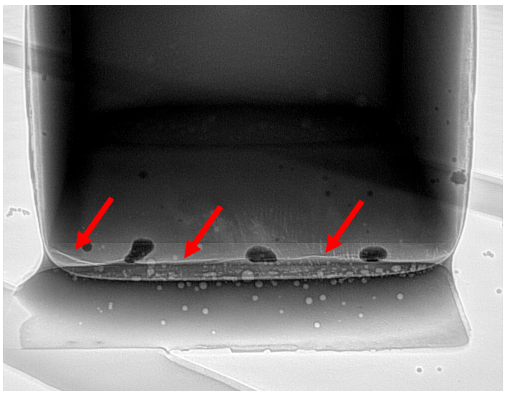

Fig. 5. X-ray image of an end termination of an 1812-sized MLCC where red arrows indicate the flex crack along the width of the capacitor.

A. *After introduction flex cracks*

Upon initial LIT measurements of all of the 24 MLCCs, the four PCBAs were bent to 6000 μStr in order to introduce flex cracks [13]. X-ray imaging was done to confirm the presence of cracks in all of the MLCCs and one example can be seen in Fig. 5 with the flex crack indicated with red arrows at the different positions. After the introduction of flex cracks was confirmed by X-ray imaging, all boards were measured again with LIT. An example of a damaged 1812-sized MLCC is shown in Fig. 6. Similarly to the case of an undamaged MLCC (Fig. 4), no hotspots can be observed and the temperature increase of approximately 5 mK is in the same range as before the bending test.

This article has been accepted for publication in a future issue of this journal, but has not been fully edited. Content may change prior to final publication. Citation information: DOI 10.1109/JESTPE.2018.2866545, IEEE Journal of Emerging and Selected Topics in Power Electronics

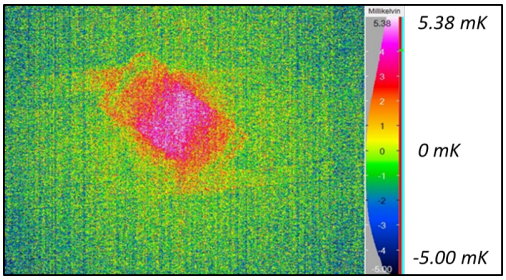

Fig. 6. Thermal footprint of a cracked 1812-sized MLCC with a temperature increase of 5 mK in the capacitor body. LIT was conducted with a lock-in frequency of 1 Hz at 10 V for 3 min. No hotspot can be detected.

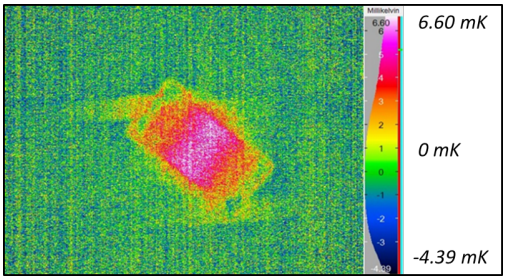

Fig. 7. Thermal footprint of a cracked 1812-sized MLCC after 24 hours THB exposure with a temperature increase of 6 mK in the capacitor body. LIT was conducted with a lock-in frequency of 1 Hz at 10 V for 3 min. No hotspot can be detected.

B. After temperature, humidity and bias

In order to accelerate the failure mode of leakage paths through the flex crack between opposing electrodes, the samples were initially submitted to 24 hours of THB. After this initial THB stress, no significant difference in the thermal footprints could be seen compared to before THB (see Figs. 7 and 6), indicating that a sufficient leakage path has not yet been formed. However, after a total of 96 hours of exposure to THB, a significant change of heating is seen in one of the 1812-sized MLCCs (see Fig. 8). In this particular case, the leakage path is large enough that it even can be measured electrically to 220 mA when 10 V DC is applied. ~~However, given some of the complex circuits on a real PCBA, LIT presents a valuable method for leakage detection through hotspot identification and analysis.~~ The hotspot shows a significant temperature increase of 373 mK, as compared to the maximum temperature increases of approximately 7 mK for all the previously measured MLCCs without any hotspots. The negative temperature differences, as indicated by the blue line corresponding to the copper trace, are due to the lock-in measurement method, namely caused by cooling which is lagging in the integration process.

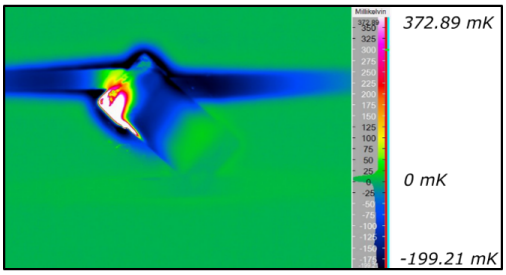

Fig. 8. Thermal footprint of a cracked 1812-sized MLCC after 96 hours of exposure to THB. A hotspot is found in the edge of the MLCC with a temperature increase of 373 mK. LIT was conducted with a lock-in frequency of 1 Hz at 10 V for 3 min.

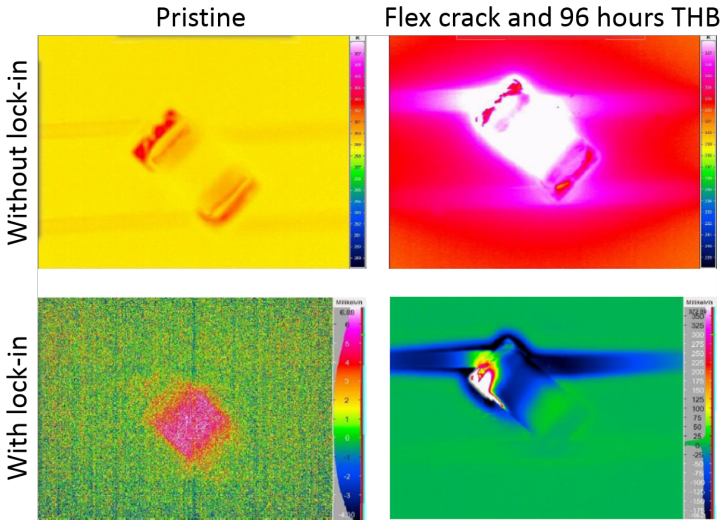

Fig. 9. Thermal footprint of a pristine as well as cracked and 96 hours of THB exposed 1812-sized MLCC using both steady-state and lock-in thermography. LIT was conducted with a lock-in frequency of 1 Hz at 10 V for 3 min.

As can be seen in Fig. 8, it is possible to detect the hotspot due to flex cracking of MLCCs after THB stress using LIT. While leakage measurements can be easily conducted for individual MLCCs, LIT measurements are advantageous for the cases where multiple MLCCs should be analyzed and evaluated at the same time. Also LIT is able to yield information as to where inside the MLCC the point of failure is located.

C. Effect of lock-in

An advantage with lock-in thermography is that it enables spatial location of the source of the hotspot, as e.g. to the left corner of the MLCC in the present example (see Fig. 8). This is not the case in standard thermographic images, where it is not possible to extract this location

as the overall heating of the component is dominant. In Fig. 9 a comparison of steady-state IR and lock-in thermography is shown, where the thermal footprint of a pristine MLCC, as well as the MLCC with a flex crack and 96 hours of THB are compared. Using standard thermography the thermal footprint of the pristine MLCC shows a temperature difference due to emissivity and focus of the camera. LIT enables identification of the active area of the pristine MLCC by removing continuous heating. The thermal footprint of the cracked and 96 hours of THB exposed MLCC indicates a hotspot, however, the source of heating cannot be identified. When using lock-in thermography this effect does not occur, because the temperature difference due to emissivity is suppressed for the pristine MLCC and the source of heating in the damaged MLCC can easily be located to the left corner.

D. Dependency on lock-in frequency

In order to learn more about the flex cracked MLCC which was exposed to 96 hours of THB, the dependency on lock-in frequency on the thermal image was investigated. Ideally, the spatial resolution should increase as the lock-in frequency is increased [18]. However, an increase in the lock-in frequency should also lead to a lower peak change in temperature, hence a small hotspot might not be detectable [15]. While the inital measurements were performed using a lock-in frequency of 1 Hz and a bias of 10 V for 3 min (see Fig. 8), in Fig. 10(a)-(c) the LIT measurement for the failed MLCC is shown for the case of a lock-in frequency of 0.1 Hz, 5 Hz, and 10 Hz, respectively. In all three thermal footprints it is seen that when the frequency is increased, the temperature of the different parts of the MLCC gets more well-defined. The spatial resolution was improved for higher frequencies in accordance with the findings in literature [15], [18]. Further, it is also seen that as the frequency increases, the corresponding peak change in temperature decreases which is also in agreement with the literature [15]. The majority of the temperature scale is negative at the measurement performed at 5 Hz due to the delay of the heating compared to the applied power.

E. Dependency on lock-in voltage

It was also investigated whether the hotspot is still visible when decreasing the bias voltage. In general, the hotspot gets stronger and is easier to detect when a larger voltage is applied. However, it is desired to use an as low as possible bias voltage, because a high bias current might damage the MLCC [10]. An approach is therefore to reduce the bias voltage once the hotspot

This article has been accepted for publication in a future issue of this journal, but has not been fully edited. Content may change prior to final publication. Citation information: DOI 10.1109/JESTPE.2018.2866545, IEEE Journal of Emerging and Selected Topics in Power Electronics

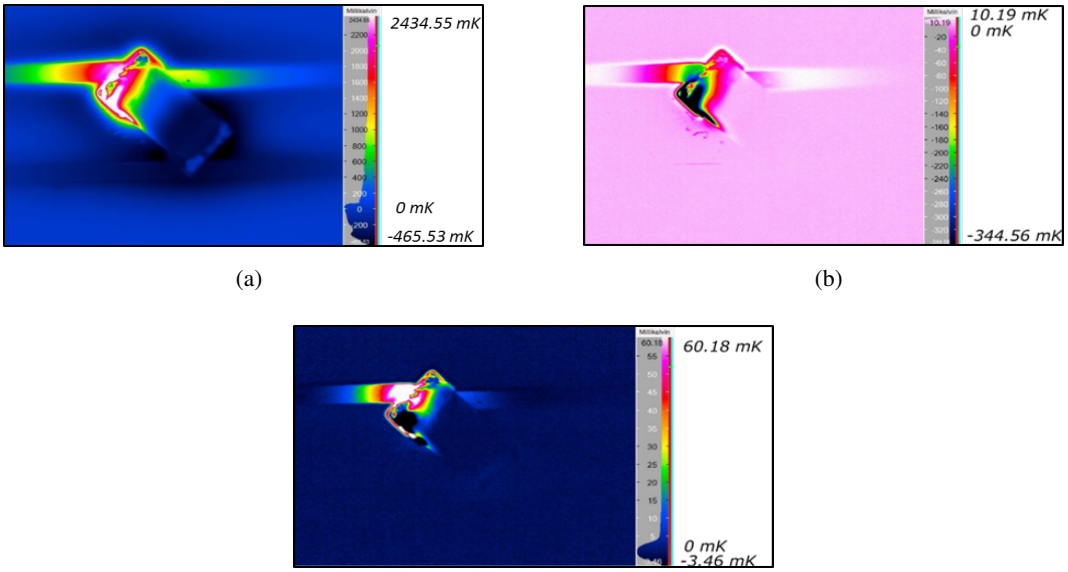

(a) (b)

(c)

Fig. 10. Thermal footprint of the failed 1812-sized MLCC shown in Fig. 8 using a lock-in frequency of (a) 0.1 Hz, (b) 5 Hz and (c) 10 Hz instead of 1 Hz. The temperature difference is negative in (b) due to the delay of the heating compared to the applied power. A measurement time of 3 min and a bias voltage of 10 V was used.

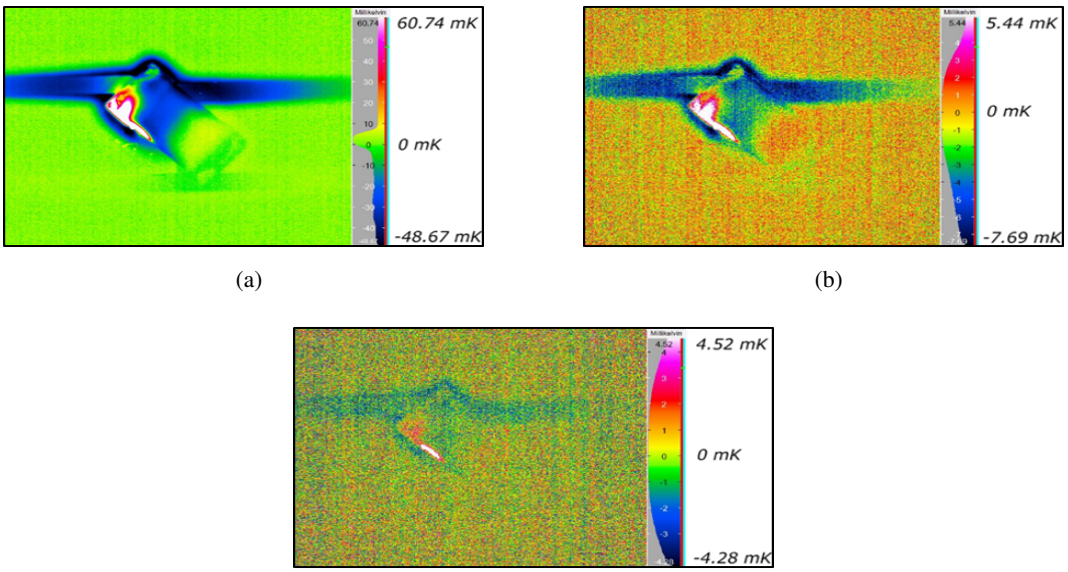

(a) (b)

(c)

Fig. 11. Thermal footprint of the failed 1812-sized MLCC shown in Fig. 8 using a bias voltage of (a) 5 V, (b) 2 V and (c) 1 V instead of 10 V. A measurement time of 3 min and a frequency of 1 Hz was used.

has been detected. By doing so, the hotspot gets smaller and the location of the fault can more easily be spotted from the resulting images. This can be an advantage if LIT is used as a tool to identify the point of investigation for other testing methods, such as e.g. optical microscopy of cross-sections, where only a small part of the sample at a certain depth can be investigated. While the initial measurements were performed at $10\ \mathrm{V}$, also lower voltages of $5\ \mathrm{V}$, $2\ \mathrm{V}$, and $1\ \mathrm{V}$ were applied. Results are shown in Fig. 11. From these figures, it is seen that the area of the hotspot is decreased as the bias voltage is decreased. Also the spreading of the heating is decreased as the supply voltage is lowered. These images can be used to identify the exact source of the hotspot in order to allow further investigations using other failure analysis methods. Using a bias of $1\ \mathrm{V}$ (see Fig. 11(c)), the hotspot region at the left corner is indicated in red, however, it is observed that there is a source of heating at the long edge of the capacitor which is indicated by the white color. The temperature difference in Fig. 11(c) is substantially lower than for higher bias voltages and instead comparable to the analysis of the pristine components (see Fig. 4). Therefore, the resolution enables only an approximate location of the leakage source.

F. Dependency on lock-in time

While it was initially seen that a hotspot could be detected by LIT using $3\ \mathrm{min}$ measurement time (Fig. 8), it is also of interest to see whether a hotspot could also be detectable with shorter measurement times. Therefore, in Fig. 12(a), a measurement time of $1\ \mathrm{min}$ is investigated. It is shown that while the temperature of the background temperature is less detailed, the hotspot is still clearly defined. Similar conclusions can be drawn from the thermal footprints in Figs. 12(b) and 12(c), which are the results of a measurement time of $30\ \mathrm{s}$ and $10\ \mathrm{s}$, respectively. While the background is less clearly defined, the hotspot is still well detectable indicating that the screening for leakage paths could be done in a fast way. As LIT is based on integration time frames, the minimal measurement time is limited in order to receive a meaningful result as any data captured before the sample has reached a thermal equilibrium will disturb the final picture.

G. Physical characterization

To verify the position of the flex crack as well as examine the origin of the hotspot, a cross-section of the MLCC was prepared. Fig. 13 depicts an image recorded by optical microscopy where several cracks can be observed in the lower left corner and another crack can be seen crossing the MLCC in parallel with the electrodes close to the bottom passive area. Some of

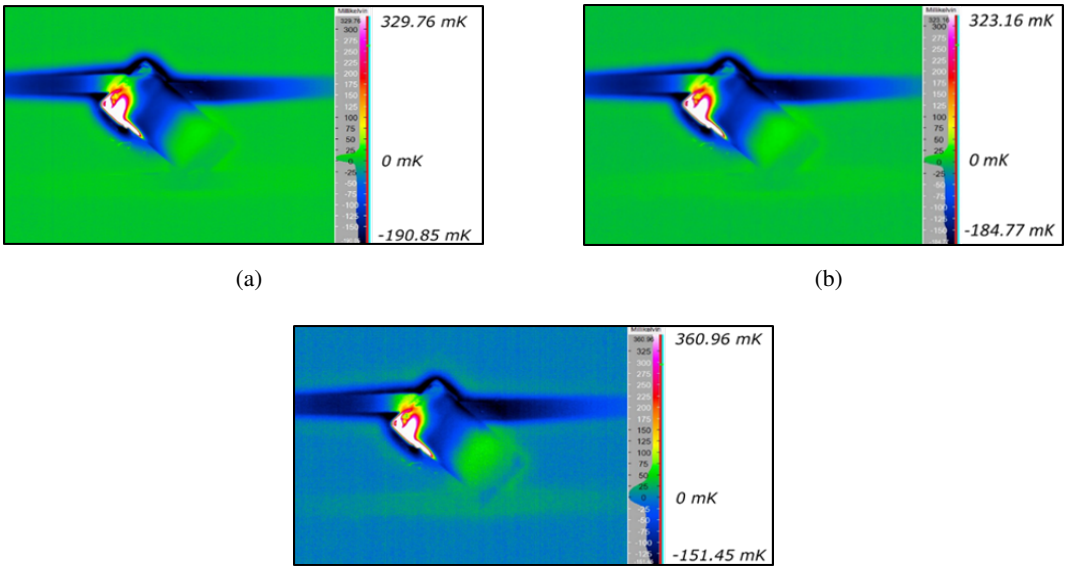

Fig. 12. Thermal footprint of the failed 1812-sized MLCC shown in Fig. 8 using a measurement time of (a) 1 min, (b) 30 s and (c) 10 s instead of 3 min. A measurement frequency of 1 Hz and bias voltage of 10 V was used.

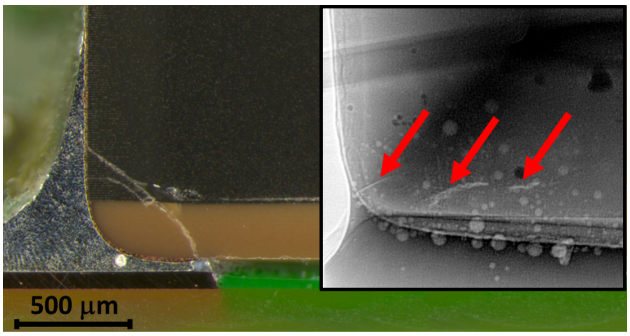

Fig. 13. Cross-section of the cracked 1812-sized MLCC after 96 hours of exposure to THB. Several cracks can be observed in the lower left corner and one crack can be seen crossing the MLCC parallel to the electrodes. Inset: X-ray image of the cracked 1812-sized MLCC with three micro cracks indicated by red arrows.

the cracks can also be seen in the X-ray image (see inset in Fig. 13), which was mirrored vertically to enable easier comparison with the cross-section. The cross-section was prepared so that the area with the three cracks (see Fig. 13) depth-wise corresponds to the area of the hotspot as indicated by LIT (left corner in Fig. 8). When the area in vicinity of the cracks in Fig. 13 is examined in more detail, it is seen that a region in the active area shows voids as well as spheres instead of the usual nickel electrode and ceramic layers (see Fig. 14). The inset of Fig. 14 shows a close-up of the area where it is seen that in addition to voids in the ceramic also

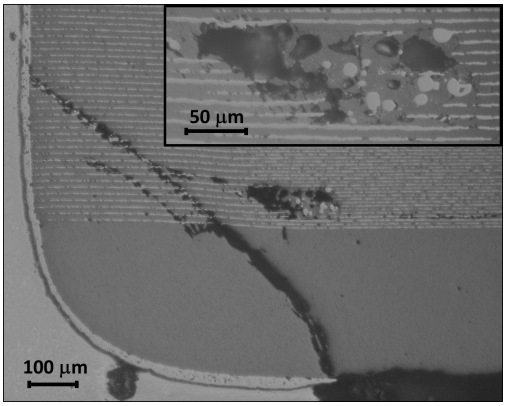

Fig. 14. Cross-section of the cracked 1812-sized MLCC shown in Fig. 13. Inset: Close-up of the area where spheres are formed out of the nickel electrodes and large voids are observed.

interruptions and spheres in the nickel electrodes are present. The shape of the nickel spheres indicate melting and solidifying of the nickel material which corresponds well with the increased local temperatures from the lock-in thermography hotspot analysis.

IV. Discussion

From the 24 cracked MLCCs which were examined with LIT after 96 hours of THB, only one of the MLCCs was found to be leaky and a hotspot could be detected. Even though flex cracks were found by X-ray imaging in all of the examined MLCCs, no hotspots were detected in the remaining capacitors. This is most probably due to the height of the flex cracks. In order to be able to form a leakage path and hotspot, a flex crack has to reach the active area so that a possible short can make a path between the overlapping electrodes. In the X-ray images of all the other MLCCs it was found that the cracks were too low to reach the above stated area. Subsequently, MLCCs where the height of the bottom passive area or distance between the end termination and the electrodes from the opposite side is lower, the probability of a crack which is able to form a leakage path and hotspot increases. In the case of the 24 MLCCs which were examined in this paper, only the one leaky sample where a hotspot could be found by LIT displayed a sufficiently high flex crack to enter in the active area.

In the cases where the flex cracks and THB treatment could create a leakage path, the lock-in parameters need to be varied in order for the hotspot to be imaged in an appropriate manner. The advantages and disadvantages of increasing the lock-in parameters, namely lock-in frequency, voltage and time, for analysis of MLCCs as described in this paper are listed in Tab. I. For

TABLE I

SUMMARY OF ADVANTAGES AND DISADVANTAGES FOR CHANGES IN LOCK-IN FREQUENCY, VOLTAGE AND TIME SPECIFIC FOR MLCC FAILURE ANALYSIS.

Parameter	**Advantages and disadvantages**
Increase of lock-in frequency	+ Higher spatial resolution - Lower peak change in temperature $\rightarrow$ small hotspot might not be detectable
Increase of lock-in voltage	+ Hotspot gets stronger and easier to detect - Further damage of MLCC possible
Increase of lock-in time	+ Suppression of disturbance caused by non-thermal equilibrium at the starting point of measurement + Suppression of statistical noise + More clearly defined background temperature - Longer measurement times needed

sampling, the lock-in frequency should be kept low in order to detect small hotspots as in this situation the detection of a hotspot is more important than spatial resolution. Once the hotspot is detected, this parameter can be changed to receive a better resolution. Also, a lower lock-in voltage is essential to prevent failure caused by the method so that it remains non-destructive. This is essential for successful root cause analysis. The detectability of a hotspot when using different lock-in measurement times is also considered. The choice of the total measuring time of the investigation is a trade-off between two conditions. On one hand, any data captured before the sample has reached a thermal equilibrium will disturb the final picture. Also, an increase in the measurement time will enhance the suppression of statistical noise, hence a hotspot will be more easily detectable. On the other hand, an increase of the lock-in time increases the investigation time, and it should therefore be considered if the increase in time is necessary to achieve the desired result. This could especially be critical when the method is used as a first screening tool in failure analysis. Overall, it is generally better for the image resolution to use a longer measurement time.

As compared to the previous work done with LIT measurements of leaky MLCCs [11], [12], an

increased resolution of lock-in thermography is added as well as a link to the leakage associated with melting and solidifying of nickel. All other analyzed samples where flex cracks were detected with X-ray measurements did not show any hotspots in LIT measurements or spherical nickel particles in the active area of the MLCCs after cross-sectioning. Because a leakage between overlapping electrodes is needed in order to detect a hotspot by LIT, the method has its highest potential as use in root cause analysis for failed MLCCs where a non-destructive failure analysis method is needed.

V. Conclusion

This paper describes how lock-in thermography can be applied to successfully detect MLCCs that have failed as a short circuit due to a flex crack after acceleration with THB conditions. The influence of the different measurement parameters on the detectability of the hotspot was investigated. Using a higher lock-in frequency results in a higher spatial resolution, however, there is a lower peak change in temperature which may lead to LIT failing to detect small hotspots. An increase of the lock-in voltage makes the hotspots more easily detectable, however, involves the danger of damaging the component. While it is seen that the background is less detailed, it is concluded that the hotspot is still well detectable with a low measurement time of $10\ \mathrm{s}$, making it promising as a fast screening method for failure analysis. Information about the location of the flex cracks and resulting hotspot from the created leakage path give important insights about the failure mechanisms, e.g. location of the cracked MLCC on the PCBA, which in turn can give information to circuit designers about where a soft/flex end termination could be used if the problem is reoccurring. Another advantage with LIT over standard thermography is that the steady state background heating is removed, which enables hotspot detection even in the presence of hot components near the cracked MLCC. The cross-section analysis confirms both the existence and the location of the flex cracks and leakage path as detected with LIT. Even though the leakage path could be detectable by leakage current measurement, LIT has the significant advantage of identifying the location of the hotspot in a non-invasive way. On a PCB all components can be scanned using LIT quickly, whereas a leakage current measurement for all components on a PCB is not realistic.

Further experiments are needed in order to provide statistics on detection of flex cracks in MLCCs with lock-in thermography. Subsequently, this method may be usable for other components.

ACKNOWLEDGMENT

The authors would like to thank the Failure Analysis team at ABB Drives in Helsinki, Finland for granting access to their X-ray machine.

REFERENCES

[1] M. J. Pan and C. A. Randall, "A brief introduction to ceramic capacitors," *IEEE Electrical Insulation Magazine*, vol. 26, pp. 44–50, 2010.

[2] D. Liu and M. J. Sampson, "Some aspects of the failure mechanism in BaTiO3-Based multilayer ceramic capacitors," in *CARTS International*, (Las Vegas), 2012.

[3] M. H. Azarian, M. Keimasi, and M. G. Pecht, "Non-Destructive techniques for detection of defects in multilayer ceramic capacitors," in *Components for Military and Space Electronics Conference and Exhibition*, 2006.

[4] F. Yeung and Y. C. Chan, "Electrical failure of multilayer ceramic capacitors caused by high temperature and high humidity environment," in *Electronic Components and Technology Conference*, 1994.

[5] Y. C. Chan and F. Yeung, "Electrical failure of multilayer ceramic capacitors subjected to environmental screening testing," *IEEE Transactions on Components, Packaging, and Manufacturing Technology*, vol. 19, no. 2, pp. 138–143, 1996.

[6] M. Keimasi, M. H. Azarian, and M. G. Pecht, "Flex cracking of multilayer ceramic capacitors assembled with Pb-Free and tin-lead solders," *IEEE Transactions on Device and Materials Reliability*, vol. 8, no. 1, pp. 182–192, 2008.

[7] G. Vogel, "Avoid flex cracks in ceramic capacitors: Analytical tool for reliable failure analysis and guideline for positioning cercaps on PCBs," *Microelectronics Reliability*, vol. 55, no. 9-10, pp. 2159–2164, 2015.

[8] N. Blattau, D. Barker, and C. Hillman, "Lead free solder and flex cracking failures in ceramic capacitors," in *Proceedings of the capacitor and resistor technology symposium*, (San Antonio, Texas), 2004.

[9] S. Levikari, T. J. Kärkkäinnen, C. Andersson, J. Tamminen, and P. Silventoinen, "Acoustic phenomena in damaged ceramic capacitors," *IEEE Transactions on Industrial Electronics*, vol. PP, no. 99, 2017.

[10] F. Gonnet, J. C. Clément, J. Perraud, and D. Carisetti, "New I.R. thermography methodology for failure analysis on tantulum capacitors." Presented at the 26th ESREF, Toulouse, France, 2015.

[11] K. K. Ng and M. Rajaratnam, "Failure analysis on multilayer ceramic capacitor (MLCC) with leakage failure caused by silver (Ag) migration in molded plastic package," in *2012 19th IEEE International Symposium on the Physical and Failure Analysis of Integrated Circuits*, pp. 1–6, July 2012.

[12] Z. Wang, "A study of low leakage failure mechanism of X7R multiple layer ceramic capacitor (MLCC)," in *ISTFA 2006: Conference Proceedings from the 32nd International Symposium for Testing and Failure Analysis (ASM International)*, pp. 142–146, November 2006.

[13] C. Andersson, E. Varescon, J. Ingman, and M. Kiviniemi, "Detection of flex cracks in multilayer ceramic capacitors by X-ray imaging," *Microelectronics Reliability*, vol. 64, pp. 352–356, 2016.

[14] InfraTec, *User Manual: IRBIS ® 3 active online: Active Thermography Software*, January 2017.

[15] O. Breitenstein, C. Schmidt, and D. Karg, "Thermal failure analysis by IR lock-in thermography," *Microelectronics Failure Analysis Desk Reference Fifth Edition, EDFAS*, 2004.

[16] IPC/JEDEC-9702A standard, *Monotonic Bend Characterization of Board Level Interconnects*, June 2004.

[17] "Phoenix Nanomex high-resolution nanofocus X-ray inspection system." https://www.gemeasurement.com/inspection-ndt/radiography-and-computed-tomography/phoenix-nanomex, downloaded on 26.01.2017.

[18] O. Breitenstein, W. Warta, and M. Langenkamp, *Lock-In Thermography – Basics and Use for Evaluating Electronic Devices and Materials*. Springer, 2010. ISBN 978-3-642-02416-0.

Caroline Andersson (M'10) was born in Sweden in 1983. She received the M.Sc. degree from the faculty of engineering at Lund University (LTH) in Sweden, and the Ph.D. from the Swiss Federal Institute of Technology (ETH) in Zurich, Switzerland. She is currently working as a senior scientist at ABB Corporate Research Center in Baden-Dättwil, Switzerland on the topic of reliability of power electronics. The main focus of her research area is accelerated life testing, physics of failure and reliability of electronics components and systems.

Ole Kristensen was born in Denmark in 1993. He received the B.Eng. and the M.Eng. degree in Power Electronics and Drives from Aalborg University, Denmark, in 2015 and 2017, respectively. His research interests include control of power converters and reliability of power electronic components.

Stefanie Miller (S'17) was born in Germany in 1992. She received the B.Sc. degree from the Swiss Federal Institute of Technology (ETH) in Zurich, Switzerland in 2017. She is currently working towards the M.Sc. degree in Physics at ETH.

Thomas Gloor was born in Switzerland in 1984. He received the B.Sc. degree from the University of Applied Sciences and Arts Northwestern Switzerland (FHNW), from University Haute-Alsace (UHA) in France and from Baden-Wuerttemberg Cooperative State University (DHBW) in Germany. He is currently working as customer quality project manager at ABB Semiconductors in Switzerland.

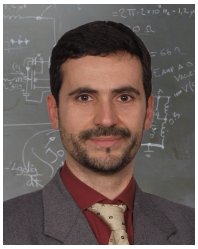

Francesco Iannuzzo (M'04–SM'12) was born in 1972. He received the M.Sc. degree in Electronic Engineering and the Ph.D. degree in Electronic and Information Engineering from the University of Naples, Italy, in 1997 and 2001, respectively. He is primarily specialized in power device modelling.

He is currently a professor in Reliable Power Electronics at the Aalborg University, Denmark, where he is also part of CORPE (Center of Reliable Power Electronics). His research interests are in the field of reliability of power devices, including mission-profile based lifetime estimation, failure modelling and testing up to MW-scale modules under extreme conditions, like overvoltage, overcurrent, overtemperature and short circuit. He is author or co-author of more than 130 publications on journals and international conferences and one patent. Besides publication activity, over the past years he has been invited for several technical seminars about reliability in first conferences as EPE, ECCE, PCIM and APEC.

Prof. Iannuzzo was the Technical Programme Committee co-Chair in two editions of ESREF, the European Symposium on Reliability of Electron devices, Failure physics and analysis. He is a senior member of the IEEE (Reliability Society, Electron Device Society, Industrial Electronic Society and Industry Application Society) and of AEIT (Italian Electric, Electronic and Telecommunication Association). He has been guest editor for Microelectronics Reliability and permanently serves as peer reviewer for several conferences and journals in the field, like: APEC, ECCE, EPE, ESREF, IECON, ISIE, Elsevier Microelectronics Reliability, IEEE Transactions on Industrial Electronics, Power Electronics and Electron Devices. Prof. Iannuzzo has been appointed ESREF 2018 general chair.